Electronic Supplementary Information for:

A general strategy to prepare macro-/mesoporous materials from thermoplastic elastomer blends

Anthony Griffin,[1] Mark Robertson,[1] Parker Frame,[1] Guorong Ma,[1] Kevin A. Green,[1] Zhiqian Han,[2] Sarah E. Morgan,[1] Xiaodan Gu,[1] Meng Wang,[2] Zhe Qiang[1,*]

[1]School of Polymer Science and Engineering, The University of Southern Mississippi, Hattiesburg, MS, 39406, USA

[2]Department of Civil and Environmental Engineering, University of Pittsburgh, PA, 15261, USA

Corresponding authors: Z. Q. (zhe.qiang@usm.edu)

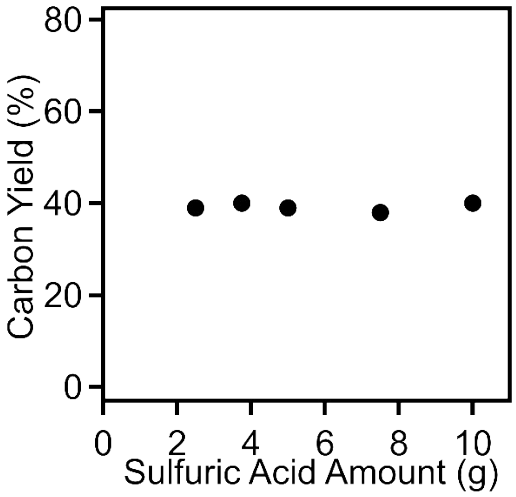

Figure S1. Carbon yield as a function of amount of sulfuric acid during the sulfonation-induced crosslinking reaction for 2 g of SIS-5.

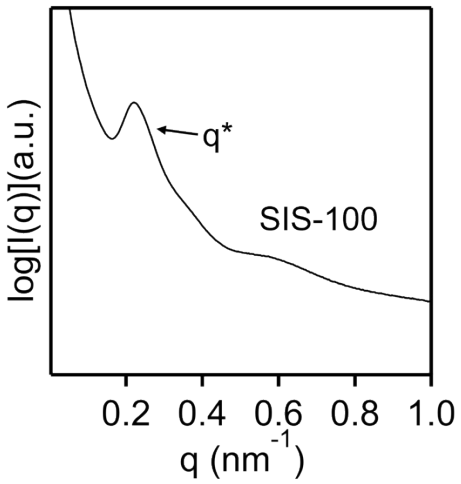

Figure S2. SAXS profile for bulk SIS.

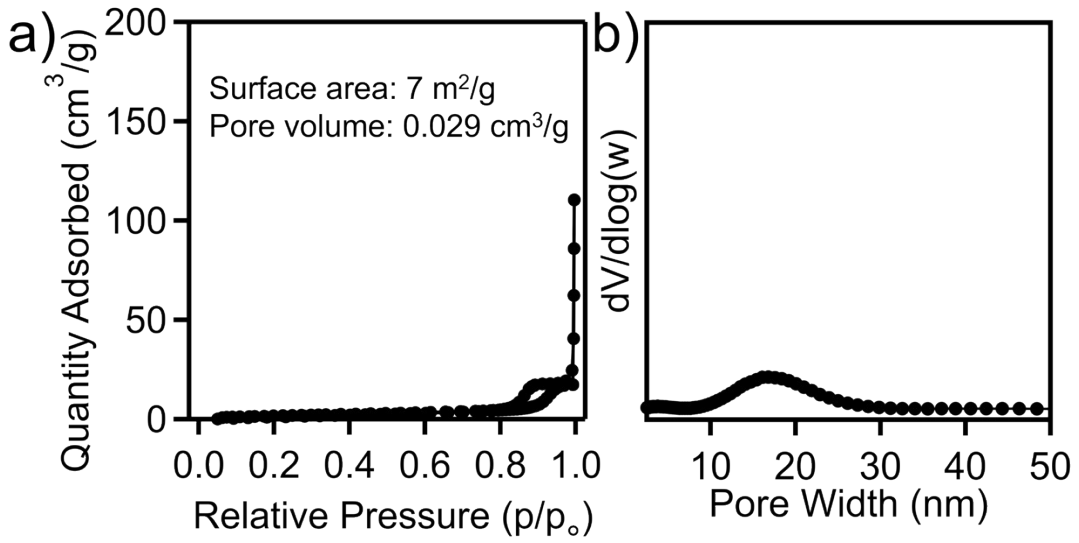

Figure S3. (a) Nitrogen adsorption isotherm and (b) corresponding pore size distribution for bulk SEBS following 12 h of sulfonation-based crosslinking at 145 °C.

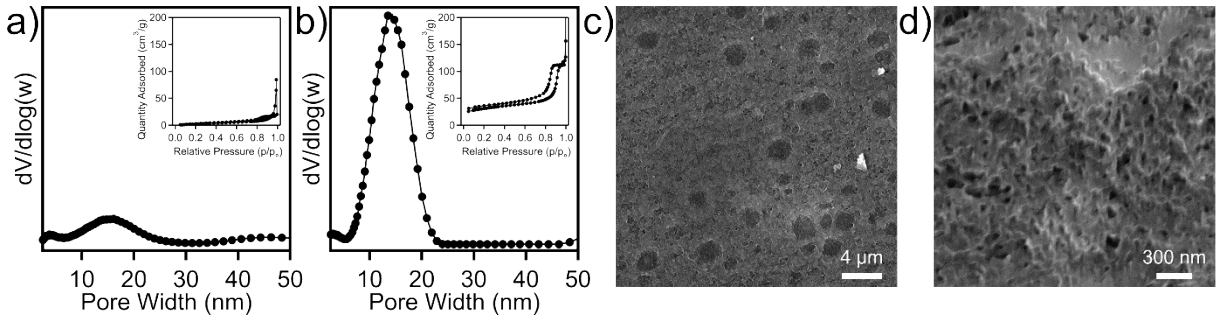

Figure S4. (a) Pore size distribution with an inset of the corresponding nitrogen adsorption isotherm of SEBS sulfonated at 145 °C for 1 h with 5 wt% PMMA. (b) Pore size distribution with an inset of the corresponding nitrogen adsorption isotherm, SEM micrographs displaying (c) macroporous and (d) mesoporous regimes of SEBS sulfonated at 145 °C for 2 h with 5 wt% PMMA.

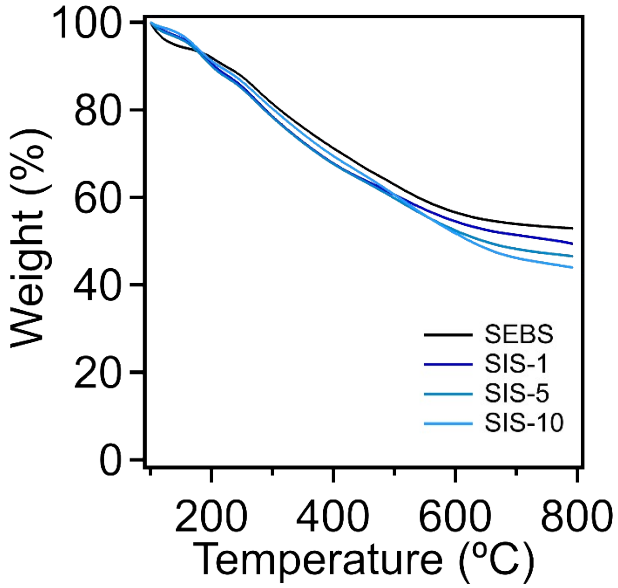

Figure S5. TGA thermograms up to 800 °C under nitrogen environment for bulk SEBS and SEBS-SIS blends sulfonated for 4 h.

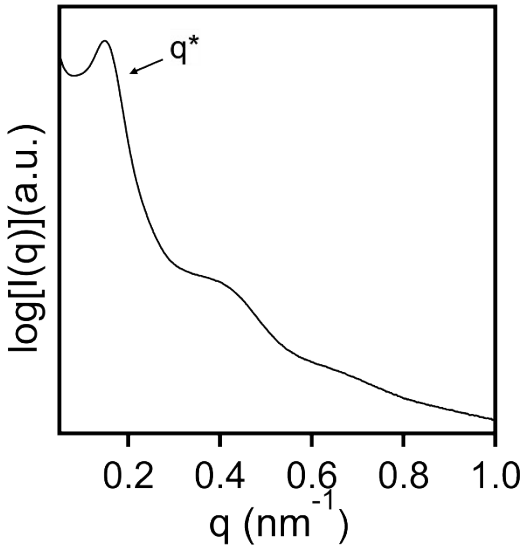

Figure S6. SAXS profiles for carbonized bulk SEBS sulfonated for 4 h.

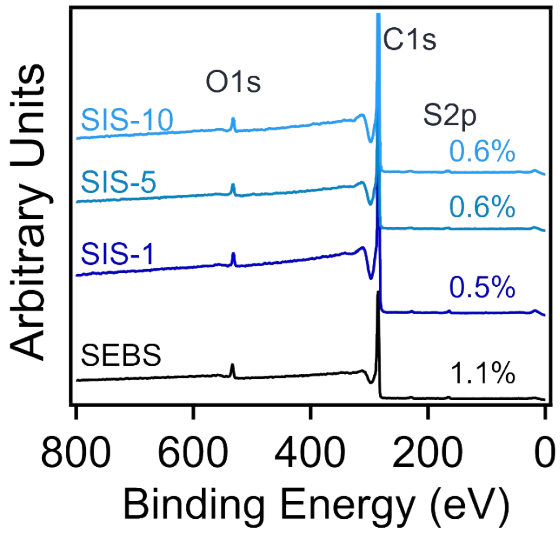

Figure S7. XPS of carbonized SEBS and SEBS/SIS blends.

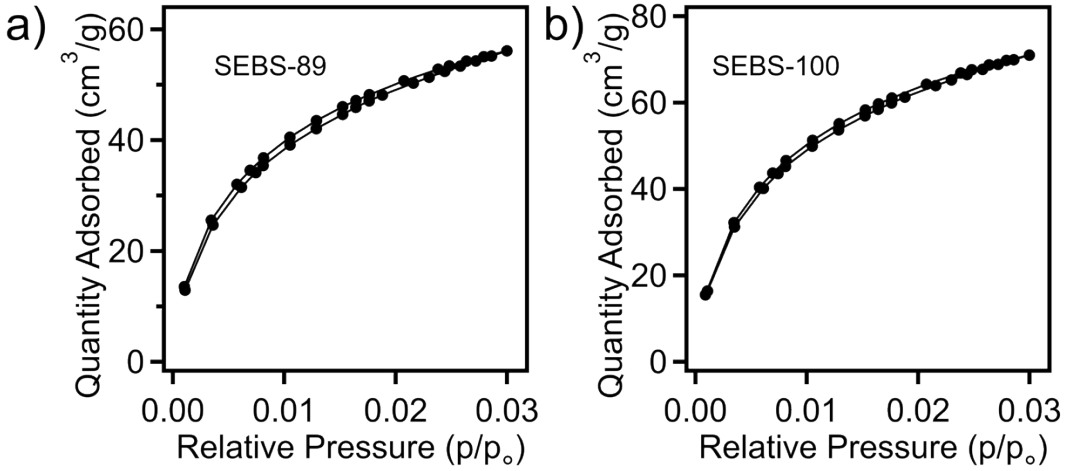

Figure S8. CO_2 adsorption isotherms for (a) SEBS-89 and (b) SEBS-100.

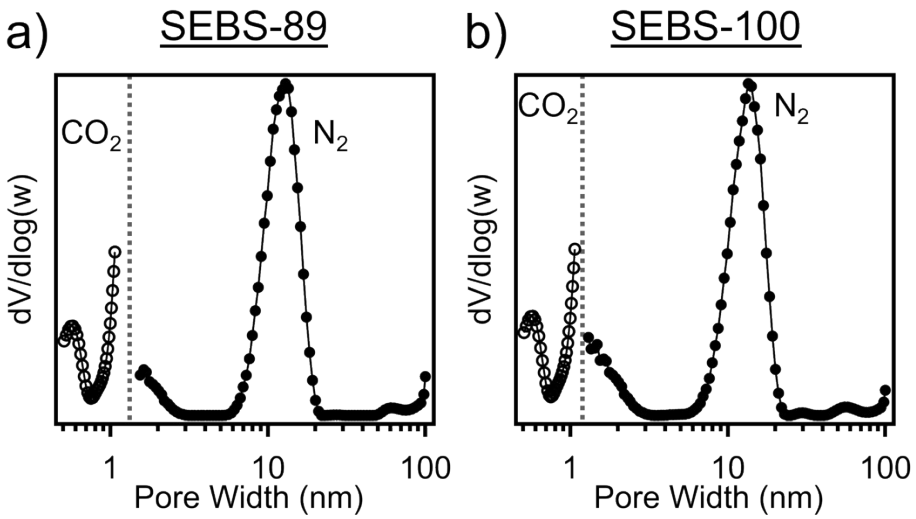

Figure S9. Pore size distributions derived from CO_2 and N_2 isotherms using NLDT of (a) SEBS-89 and (b) SEBS-100.

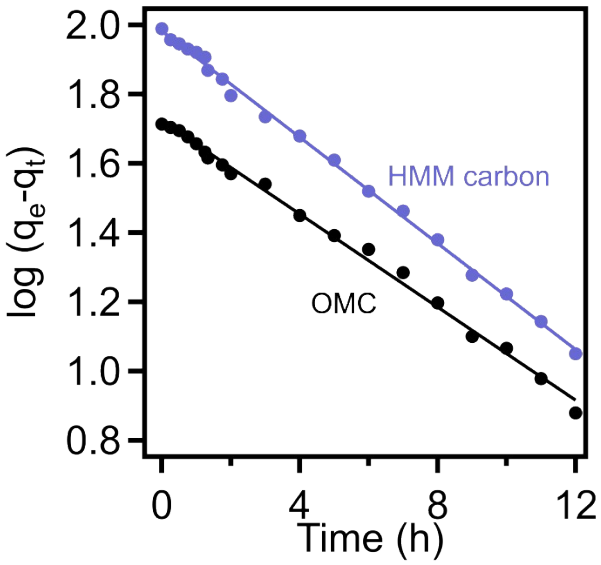

Figure S10. Pseudo first-order kinetic model fitting of adsorption kinetics at 50 mg/mL rhodamine b concentration for HMMC and an OMC control.

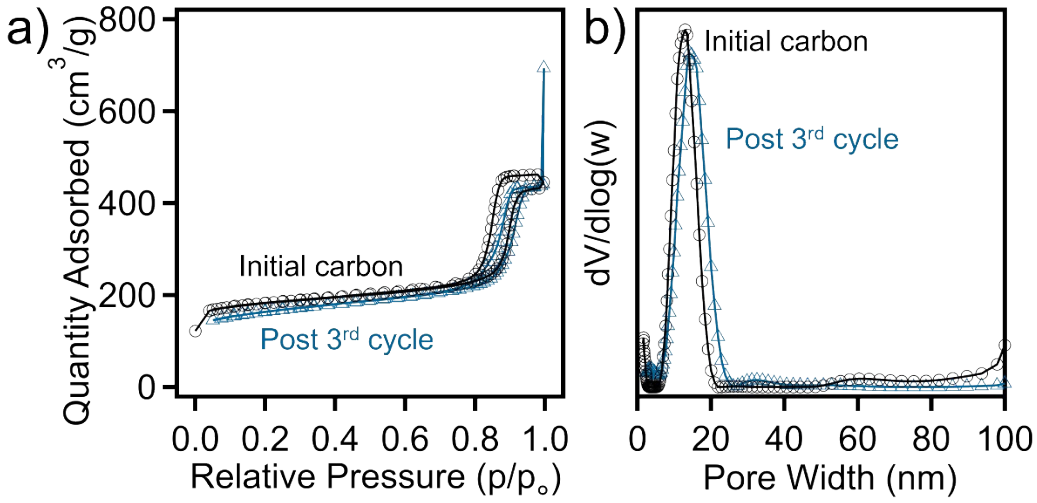

Figure S11. (a) Nitrogen adsorption isotherm and (b) corresponding pore size distribution for initial HMM carbon and carbon following regeneration after 3 cycles of dye adsorption.

Table S1. Surface roughness values for neat SEBS, SIS-1, SIS-5, and SIS-10.

Sample	R_{max} (nm)
SEBS	5.4
SIS-1	7.2
SIS-5	21
SIS-10	37

R_{max} is the largest successive value of the maximum heights within a sample length.

Table S2. HMM polymer metal adsorption isotherm parameters fit with Langmuir adsorption model.

Metal ion	q_m (mg/g)	K_L (L/mg)	R^2
Co^{2+}	49.7	0.192	0.9972
Ni^{2+}	74.9	8.42×10^{-3}	0.9904

Table S3. Comparison of Co^{2+} Langmuir adsorption isotherm parameters on HMM polymers with those of other adsorbents.

Reference	Adsorbent	Langmuir Isotherm		Equilibrium Time (min)
		Q_m (mg g^{-1})	K_L (L $mmol^{-1}$)	
This paper	HMM polymer	49.69	0.192	20
1	Crosslinked 2-aminopyridine functionalized SMA copolymer	49.02	0.1052	N/A
2	Mesoporous silica SBA-15-supported surface ion imprinted polymer	39.26	0.0494	300
2	Mesoporous silica SBA-15-supported polyethyleneimine	12.21	0.0248	300
4	Nanohydrogel tragacanth gum-g-polyamidoxime	100	0.0884	60
5	Anthranilic acid – 2-aminopyridine – formaldehyde terpolymer	3.51	0.478	N/A
6	Magnetic cobalt ion-imprinted polymer	23.09	0.053	150
6	Magnetic cobalt non-imprinted polymer	16.88	0.069	150
7	Magnetic poly(methyl methacrylate-divinylbenzene-NH_2) beads	50.3	0.252	60
8	Fe_3O_4-modified ploy(methyl methacrylate-*co*- maleic anhydride) nanocomposite	90.9	0.078	N/A

Table S4. Comparison of Ni^{2+} Langmuir adsorption isotherm parameters on HMM polymers with those of other adsorbents.

Reference	Adsorbent	Langmuir Isotherm		Equilibrium Time (min)
		Q_m (mg g^{-1})	K_L (L $mmol^{-1}$)	
This paper	HMM polymer	74.88	0.008	20
1	Crosslinked 2-aminopyridine functionalized SMA copolymer	76.52	0.044	N/A
3	Semi-Interpenetrating polyacrylamide-potato starch cryogels	9.87	0.481	N/A
5	Anthranilic acid – 2-aminopyridine – formaldehyde terpolymer	3.89	0.34	N/A
7	Magnetic polymethyl methacrylate-divinylbenzene-NH_2 beads	49.6	0.131	60
9	Polyaniline@aminopropyltriethoxysilane-Fe_3O_4/ attapulgite	142.86	0.0267	15

Table S5. Regeneration efficiency of HMM carbon for three consecutive cycles of adsorption and thermal treatment.

Cycle number	Adsorption capacity (mg/g)	Regeneration efficiency (%)
1	532	-
2	213	40
3	197	37
4	184	35

References

1 N. Samadi, R. Hasanzadeh and M. Rasad, *J. Appl. Polym. Sci.*, 2014, **132**, 41642.

2 Y. Liu, Z. Liu, J. Dai, J. Gao, J. Xie and Y. Yan, *Chin. J. Chem.*, 2011, **29**, 387–398.

3 D. F. Apopei, M. V. Dinu, A. W. Trochimczuk and E. S. Dragan, *Ind. Eng. Chem. Res.*, 2012, **51**, 10462–10471.

4 A. Masoumi and M. Ghaemy, *Carbohydr. Polym.*, 2014, **108**, 206–215.

5 R. S. Azarudeen, R. Subha, D. Jeyakumar and A. R. Burkanudeen, *Sep. Purif. Technol.*, 2013, **116**, 366–377.

6 R. Kang, L. Qiu, L. Fang, R. Yu, Y. Chen, X. Lu and X. Luo, *J. Environ. Chem. Eng.*, 2016, **4**, 2268–2277.

7 Z. Lin, Y. Zhang, Y. Chen and H. Qian, *Chem. Eng. J.*, 2012, **200**–**202**, 104–112.

8 A. Masoumi, M. Ghaemy and A. N. Bakht, *Ind. Eng. Chem. Res.*, 2014, **53**, 8188–8197.

9 P. Sun, W. Zhang, B. Zou, X. Wang, L. Zhou, Z. Ye and Q. Zhao, *Appl. Clay Sci.*, 2021, **209**, 106151.